25th IMEKO TC4 International Symposium
23rd International Workshop on ADC and DAC Modelling and Testing
IMEKO TC-4 2022
Brescia, Italy / September 12-14, 2022

Cascaded H-Bridges Multilevel Inverter Drive: Active Power Analysis in Frequency Domain

A.O. Di Tommaso[1], R. Miceli, C. Nevoloso, G. Scaglione, G. Schettino, C. Spataro

[1]*Department of Engineering, University of Palermo, Viale Delle Scienze, Building nr. 9, 90128 Palermo, claudio.nevoloso@unipa.it*

***Abstract* –The international standard IEC 61800-9-2 introduces energy efficiency classification for frequency converters or complete drive module (CDM) and provides instrumentation minimum requirements for accurate measurement of CDM input and output power valid for conventional pulse-width-modulated (PWM) voltage source inverter (VSI). This paper highlights the necessary improvements to update the standard with more detailed prescriptions according to the converter topologies and the modulation techniques adopted. In this framework, this paper address the power analysis in the frequency domain of a cascaded H-bridges-multilevel inverter (CHBMI) in an interior permanent magnet synchronous motor (IPMSM) drive for the identification of the minimum measurement bandwidth. The power spectrums are analyzed for different modulation strategies, different switching frequency values and IPMSM working conditions.**

I. INTRODUCTION

In recent years, a significant increase in global electrical energy consumption by electrical drives has been detected, with more than 47% of world electricity demand [1]-[2]. At present, most commercial electrical drives employ conventional two-level VSI for motor speed and torque control purposes. The desired output voltage is modulated by the PWM strategy, allowing motor operation at partial speed with energy-saving benefits. However, the VSI presents power losses that affect the drive overall efficiency and introduce motor additional harmonic losses [3]-[4]. Therefore, the efforts of the scientific community focused on the adoption of new solutions to optimize the electric drive performance in terms of power losses. A possible solution is the adoption of multilevel power inverters (MPIs) [5]. This technology is widely employed in traction electrical drives [6]. In automotive applications, recent studies highlight that to address long charging time and low maximum driving range issues, it is necessary to move toward higher-voltage DC links with consequent adoption of MPIs [7]. The main benefits derived by MPIs adoption can be summarized in output voltage reduced harmonic content, lower voltage stress, lower power losses and reduced electromagnetic interference (EMI) [8]-[9].

The international standards IEC 61800-9-1 [10] and IEC 61800-9-2 [11] provide the prescriptions for power losses measurement and energy efficiency classification of the power drive system (PDS), CDM and motor. The prescriptions regarding the CDM power losses measurement are defined for a conventional VSI that employs PWM or space vector modulation (SVM) strategy. No specific prescriptions are reported for other inverter topology structures. Although instrumentation minimum requirements prescriptions are general and can be applied for different inverter topologies and modulation strategies, they may be overestimated for MPIs.

This paper deals with the analysis of CHBMI input and output powers in the frequency domain. The goal is to identify the minimum instrumentation bandwidth for accurate power losses identification. Experimental analyses are performed according to IEC 61800-9-2 prescriptions on IPMSM drive fed by CHBMI. The paper is organized as follows: Section II summaries IEC 61800-9-2 main prescriptions for accurate power losses detection; Section III described the test bench, IPMSM drive fed by CHBMI and modulation strategies considered; Section IV presents the experimental results and their analysis.

II. IEC 61800-9-2 PRESCRIPTIONS

In the last decades, different regulatory bodies introduced energy efficiency classification for electrical equipment. The newest IEC 61800-9-2 introduce energy efficiency indicators IE for PDS, motor starter and power electronics systems. The standard defines three different efficiency classes IE0-IE2 for frequency converters or CDMs. The standard defines a reference CDM (RCDM) composed of a line choke, diode rectifier, DC link and output VSI for IE classification as shown in Fig. 1 [11].

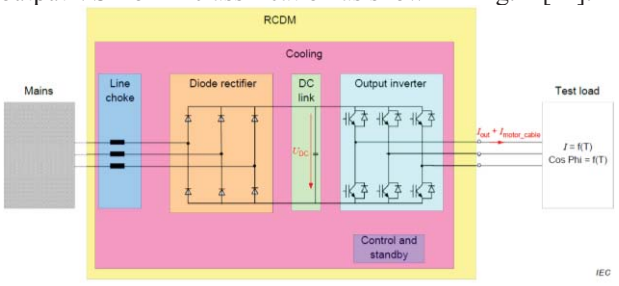

Fig. 1 RDCM and test load.

The standard can be applied for CDMs that present a

power rating range of 0.12-1000 kW, voltage range of 100-1000 V and also for CDM used in low voltage power drive systems. Three different types of testing for CDM loss determination are reported: analytical method, calorimetric method and input-output measurement method. The last method requires the measurement of electrical input and output CDM powers by employing only electrical measurement equipment and it is low time-consuming. Various power loss measurement techniques for power electronics systems, including the above described, are accurately discussed in [12]. To provide extensive loss results applicable for common electric drive applications, IEC 61800-9-2 prescribes the CDM loss measurement at partial loads as shown in Fig. 2.

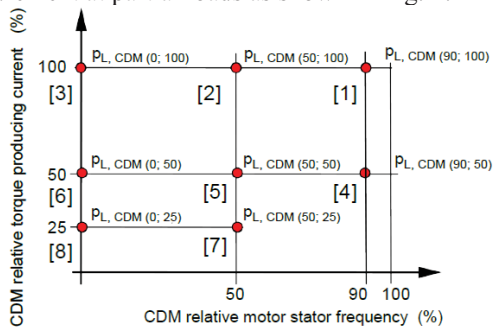

Fig. 2 CDM test point according to IEC 61800-9-2.

The standard does not specify the test load type, thus an electronic load or electric motor can be used. The CDM relative torque producing currents reported represent the minimum values and slightly higher values can be used. The torque producing current values are reported in [11] as a function of motor-rated powers. Moreover, since the VSI is responsible for most of the power losses which are a function of phase displacement between the output voltage and current fundamental components, the standard provides displacement power factor (DPF) reference values for the load as a function of motor-rated power [11]. The tests shall be conducted by the use of a power analyzer or data acquisition systems able to perform harmonic analysis. For CDM testing, a tolerance of ± 0.08 is allowed in DPF reference values. The standard also reports the reference switching frequency that is 4 kHz for CDM range power up to 90 kW and 2 kHz for CDM range power above 90 kW. On the base of the above prescriptions described, the standard provides the minimum accuracy specifications for measurement instruments used for efficiency classification. The instrumentation used for measuring power and CDM electrical quantities shall meet the requirements reported in the standard IEC 60034-2-1 [13]. The standard suggests a bandwidth at least of 10 times of VSI switching frequency.

Although the standard prescriptions are valid for traditional two-level VSI, they are not defined considering other inverter topology structures, modulation strategies and operations at higher switching frequencies. Paying attention to MPIs case, usually, the typical switching frequency adopted ranges from 5 kHz to 20 kHz with typical Multi-carrier PWM (MC-PWM) strategies [9]. Furthermore, the MPIs output voltages present reduced harmonic content with respect to traditional two-level VSIs, resulting in lower harmonic content in motor currents and consequently output power spectrum limited at lower bandwidth values. The modulation strategies adopted for motor control purpose and their control features are a function of the application and motor-rated power [6]. Therefore, traditional PWM or SVM modulations are not always adopted. The analysis related to the accurate measurement of power losses in CHBMI converters is described below.

III. IPMSM DRIVE UNDER TEST AND TEST BENCH

To perform an adequate power analysis, an IPMSM electrical drive fed by CHBMI has been set up. It is composed of a three-phase five-level CHBMI prototype (Fig. 3) whose main parameters are reported in [9] and 6 poles, three-phase IPMSM with interior SmCo magnets, whose rated mechanical speed and torque are 4000 rpm and 1.8 N·m, respectively. A Magtrol hysteresis brake (Model HD-715-8NA), connected to the shaft of the motor is used as a mechanical load. The electrical quantities are acquired by Teledyne LeCroy MDA 8028HD oscilloscope equipped with three high voltage differential probes Teledyne Lecroy HVD3106A 1 kV, 120 MHz, and three high sensitivity current probe Teledyne Lecroy CP030A AC/DC, 30 A rms, 50 MHz. The CHBMI is supplied with six DC RSP-2400 sources with 48 V of rated voltage [9].

A traditional field-oriented control (FOC) strategy, shown schematically in Fig. 4, has been implemented in PED Board FPGA control unit programmable in the Labview environment. This control strategy presents a closed-loop control of speed and currents performed by the use of PI controller. The peculiar feature of this control consists in the possibility to vary the modulation strategy adopted and its main parameter features such as the switching frequency f_{sw}. In this work, Phase Shifted (PS) and Phase Disposition (PD) modulation strategies have been considered with Sinusoidal (S) and Switching Frequency Optimal (SFO) modulating signals (Fig. 5). A detailed description of MC-PWM considered is reported in [9]. The test bench set-up is shown in Fig. 6.

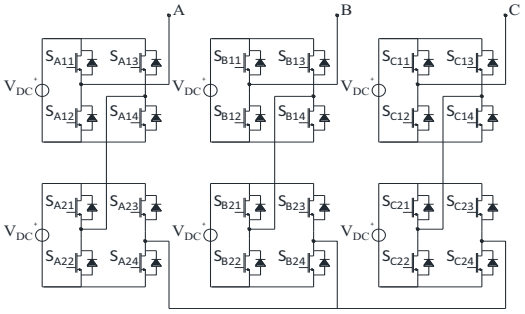

Fig. 3 Three-phase five-level CHBMI.

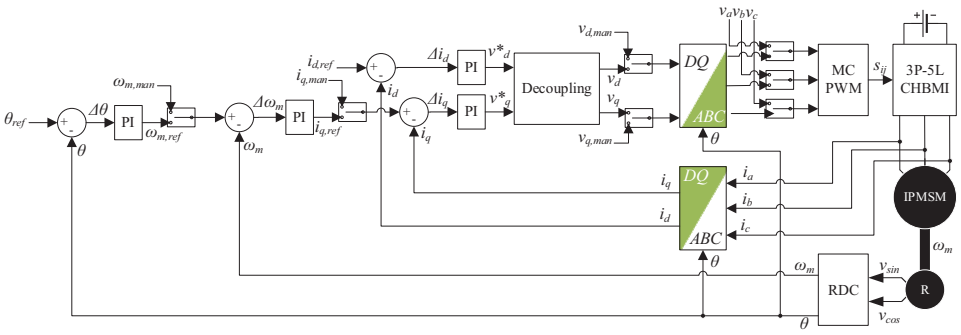

Fig. 4 FOC block diagram.

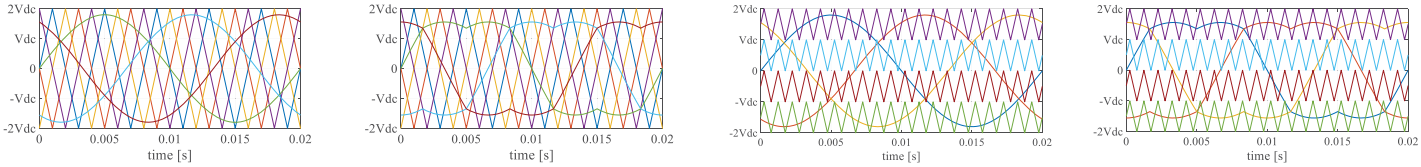

(a) (b) (c) (d)

Fig. 5 MC-PWM strategies: (a) SPSPWM, (b) SFOPWM, (c) SPDPWM, (d) SFOPDPWM.

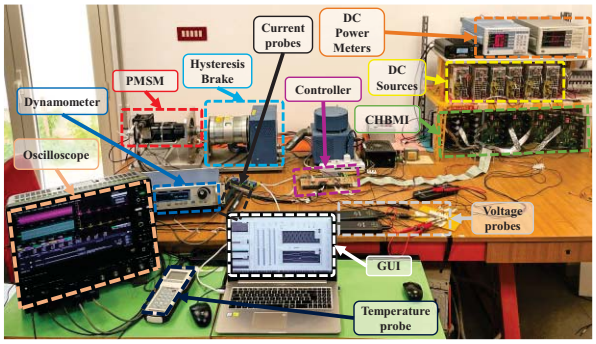

Fig. 6 Test bench.

IV. EXPERIMENTAL RESULTS

The CDM working points defined by the standard IEC 61800-9-2 (Fig. 3) plus an additional measurement point, defined at 90% of motor stator frequency and 25% of motor torque producing current, for a total of 9 measurement points, have been considered. Three different CHBMI switching frequency f_{sw} values equal to 5, 10 and 15 kHz have been considered. The sampling frequency *fs* and acquisition window have been fixed equal to 1 MS/s and 1 s, respectively. Input and output CHBMI electrical quantities have been acquired by MDA 8028HD scope and used for the determination of instantaneous power, active power and its frequency spectrum. These quantities are determined by the computational approach described in [14]. Since similar results have been obtained for all switching frequencies considered, the analysis carried out at 10 kHz is described below. The input voltage and current waveforms of CHBMI single-phase H-bridges, operating at the measurement point 1, are reported in Fig. 7 obtained with SFOPS and SFOPD strategies where the currents present double ripple frequency with respect to the fundamental CHBMI output current. Similar trends have been obtained with SPS and SPD modulation strategies. As expected, almost all of the active power is generated by the DC voltage and current components, and current harmonics generate a very small amount of active power as shown in Fig. 8 (a). The CHBMI input cumulative active power trend, expressed in percent as a function of the frequency, is reported in Fig. 8 (b).

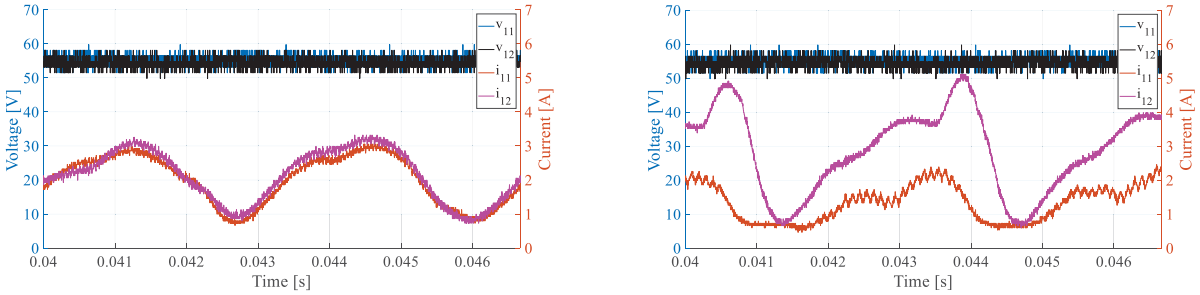

(a) SFOPS (b) SFOPD

Fig. 7 CHBMI input voltage and current waveforms of single-phase H-bridges.

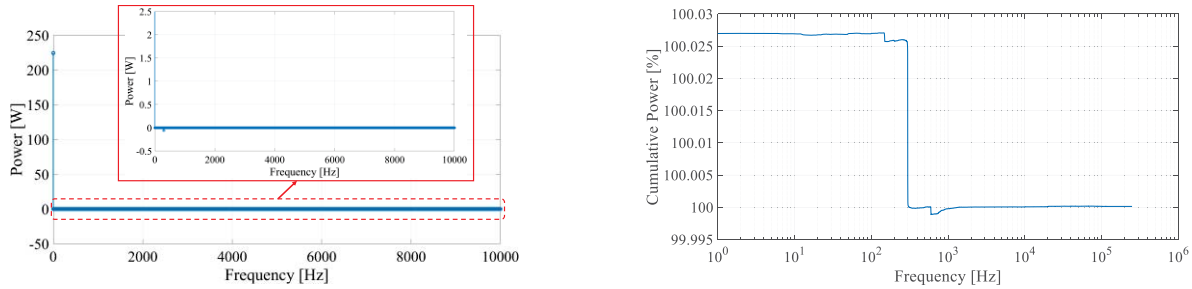

Fig. 8 CHBMI input active power spectrum (a) and cumulative power trend (b) of a single phase

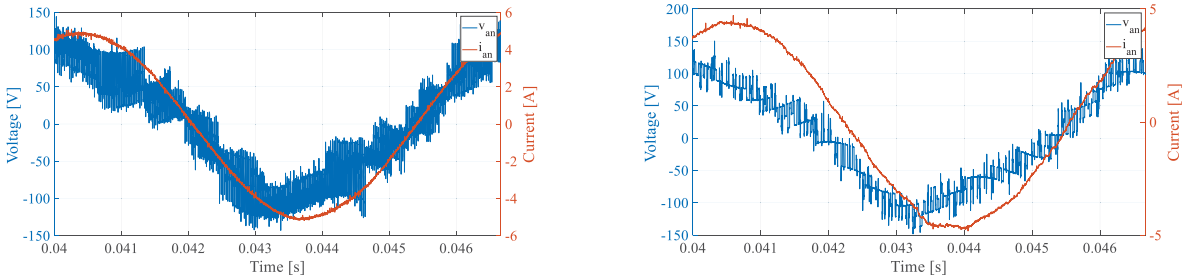

Fig. 9 CHBMI output voltage and current waveforms of a single phase.

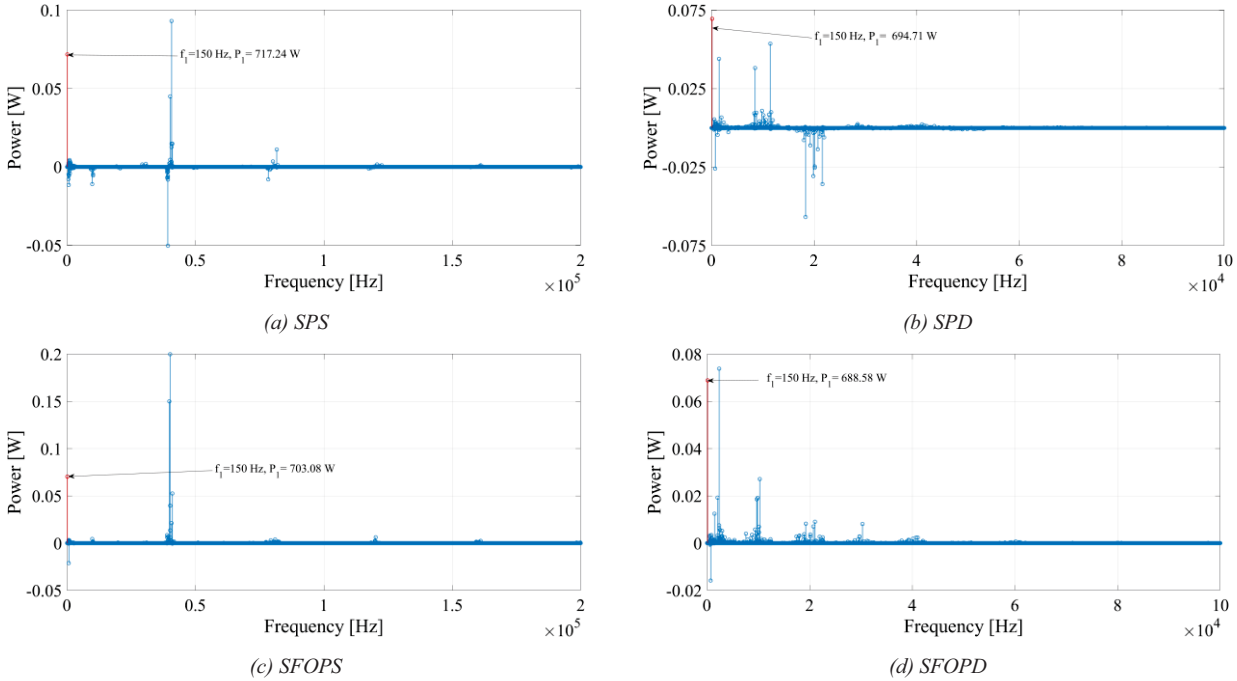

Fig. 10 CHBMI output active power spectrum.

In detail, the even current harmonics result in a small contribution of active power from the load to the power supply. This analysis highlights that it is not necessary to employ a power analyzer or transducers with a wide bandwidth for adequate active power measurement. A similar analysis has been carried out for CHBMI output section by measuring all phase voltage and current quantities. CHBMI single-phase output voltage and current waveforms, obtained for SPS and SPD strategies in correspondence to point 1, are shown in Fig. 9. In this case, CHBMI output electrical quantities have a much more significant harmonic content than CHBMI input electrical quantities. The CHBMI output voltage is affected by harmonic components that are integer

multiples of the switching frequency f_{sw} for SPD and SFOPD strategies and integer multiples of 4 f_{sw} for SPS and SFOPS [15]. To highlight the impact of voltage and current harmonics on CHBMI output active power, by way of example, the active power spectrum for CHBMI operating at measurement point 1 is reported in Fig. 10. The figure shows a zoomed view of the active power spectrum and the active power value generated by the voltage and current fundamental harmonics. It is possible to observe that the active power generated by the voltage and current harmonics presents significantly reduced amplitude compared to the fundamental one. These results are more appreciable in the cumulative active power trends as a function of the frequency reported in Fig. 11. The zoomed views show that, above the fundamental frequency, the current and voltage harmonics generate an active power contribution of less than 0.5% of total active power. Similar results have been obtained for all measurement points considered. Fig. 12 reports the percent cumulative active power trends obtained by decomposing the frequency range into three different frequency ranges: the first ranges from 0 to f_1, the second ranges from f_1 to f_{sw}-1000 Hz and the third ranges from f_{sw}-1000 to $f_s/2$. In this way, it is possible to highlight the active power contribution of fundamental quantities, the active power contribution of harmonics quantities working at a frequency lower than f_{sw} and the active power contribution of harmonics quantities working in a frequency band including f_{sw} and higher values. The results obtained with SPS and SFOPS strategies show that the fundamental quantities contribute to more than 98.5% of total active power and, below the f_{sw}, the cumulative active power presents a value higher than 99.5 % in all measurement points. Similar results have been obtained with SPD and SFOPD strategies. In some measurement points, the harmonics quantities operating at the third frequency band present an active power contribution higher than 0.6%. The analysis carried out is of considerable importance because it highlights that, to measure almost all of the active power generated by a CHBMI, it is necessary to consider the frequency bandwidth range from 0 to f_{sw}.

V. CONCLUSIONS

This paper presents an experimental active power analysis of an IPMSM drive fed by CHBMI controlled with four different modulation strategies and by considering three different switching frequencies. As expected, the analysis carried out showed that the CHBMI input power is generated by the voltage and current DC components and, therefore, it is not necessary to use power analyzers or transducers with wide bandwidth. The CHBMI output section presents more complex behaviour due to modulation strategies effects that result in not negligible voltage and current harmonic components. The analysis carried out showed that voltage and current harmonics, operating at switching frequency and higher value, contribute to the generation of active power in almost all cases below 0,6%. These results highlight that for CHBMIs, it is not necessary to choose a sampling frequency at least equal to 10 times the switching frequency as described by the standard IEC 618009-2.

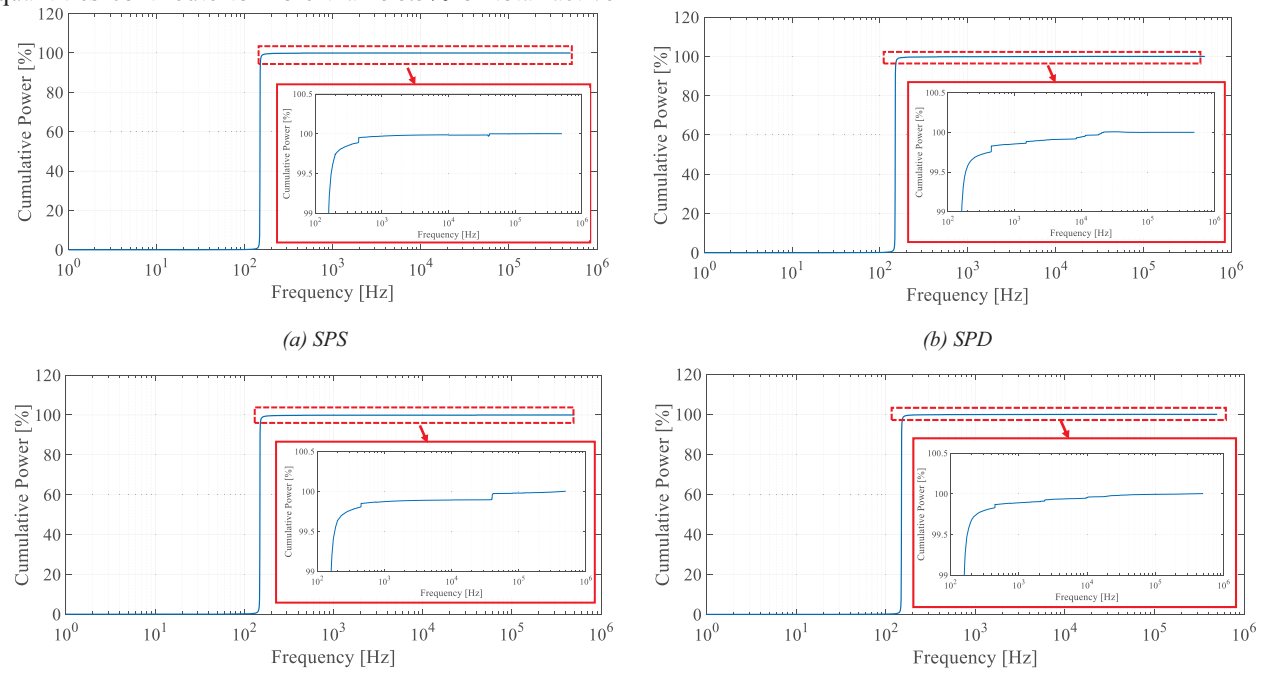

Fig. 11 CHBMI output active cumulative power trend.

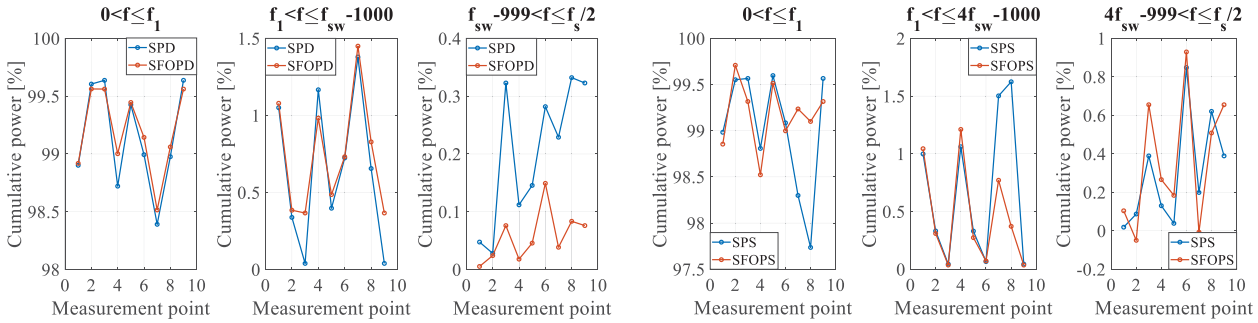

Fig. 12 CHBMI output active cumulative power values for each working point.

REFERENCES

[1] L. Aarniovuori, H. Kärkkäinen, A. Anuchin, J. J. Pyrhönen, P. Lindh and W. Cao, "Voltage-Source Converter Energy Efficiency Classification in Accordance With IEC 61800-9-2," in *IEEE Transactions on Industrial Electronics*, vol. 67, no. 10, pp. 8242-8251, Oct. 2020.

[2] V. Cecconi, V. Di Dio, A. O. Di Tommaso, S. Di Tommaso, D. La Cascia and R. Miceli, "Active power maximizing for Wind Electrical Energy Generating Systems moved by a Modular Multiple Blade Fixed Pitch Wind Turbine," *2008 International Symposium on Power Electronics, Electrical Drives, Automation and Motion*, 2008, pp. 1460-1465.

[3] Caruso, M., Di Tommaso, A.O., Miceli, R., Nevoloso, C. & Spataro, C. 2021, "Uncertainty evaluation in the differential measurements of power losses in a power drive system", *Measurement: Journal of the International Measurement Confederation*, vol. 183, 109795, ISSN 0263-2241.

[4] H. Karkkainen, L. Aarniovuori, M. Niemela and J. Pyrhonen, "Converter-Fed Induction Motor Efficiency: Practical Applicability of IEC Methods," in *IEEE Industrial Electronics Magazine*, vol. 11, no. 2, pp. 45-57, June 2017.

[5] D. Ronanki and S. S. Williamson, "Modular Multilevel Converters for Transportation Electrification: Challenges and Opportunities," in *IEEE Transactions on Transportation Electrification*, vol. 4, no. 2, pp. 399-407, June 2018.

[6] A. Poorfakhraei, M. Narimani and A. Emadi, "A Review of Modulation and Control Techniques for Multilevel Inverters in Traction Applications," in *IEEE Access*, vol. 9, pp. 24187-24204, 2021.

[7] H. Tu, H. Feng, S. Srdic and S. Lukic, "Extreme Fast Charging of Electric Vehicles: A Technology Overview," in *IEEE Transactions on Transportation Electrification*, vol. 5, no. 4, pp. 861-878, Dec. 2019.

[8] A. Poorfakhraei, M. Narimani and A. Emadi, "A Review of Multilevel Inverter Topologies in Electric Vehicles: Current Status and Future Trends," in *IEEE Open Journal of Power Electronics*, vol. 2, pp. 155-170, 2021.

[9] Busacca, A.; Di Tommaso, A.O.; Miceli, R.; Nevoloso, C.; Schettino, G.; Scaglione, G.; Viola, F.; Colak, I. Switching Frequency Effects on the Efficiency and Harmonic Distortion in a Three-Phase Five-Level CHBMI Prototype with Multicarrier PWM Schemes: Experimental Analysis. *Energies* 2022, *15*, 586.

[10] IEC 61800-9-1. Adjustable speed electrical power drive systems - Part 9-1: Ecodesign for power drive systems, motor starters, power electronics and their driven applications - General requirements for setting energy efficiency standards for power driven equipment using the extended product approach (EPA) and semi analytic model (SAM), 2017.

[11] IEC 61800-9-2. Adjustable Speed Electrical Power Drive Systems—Part 9-2: Ecodesign for Power Drive Systems, Motor Starters, Power Electronics & Their Driven Applications—Energy Efficiency Indicators for Power Drive Systems and Motor Starters, 2017.

[12] C. Xiao, G. Chen and W. G. H. Odendaal, "Overview of Power Loss Measurement Techniques in Power Electronics Systems," in *IEEE Transactions on Industry Applications*, vol. 43, no. 3, pp. 657-664, May-june 2007.

[13] IEC 60034-2-1. Rotating electrical machines - Part 2-1: Standard methods for determining losses and efficiency from test, 2014.

[14] A. Anttila, L. Aarniovuori, M. Niemelä, M. Zaheer, P. Lindh and J. Pyrhönen, "Active Power Analysis of PWM-driven Induction Motor in Frequency Domain," *2021 XVIII International Scientific Technical Conference Alternating Current Electric Drives (ACED)*, 2021, pp. 1-6.

[15]S. Benanti *et al.*, "Experimental analysis with FPGA controller-based of MC PWM techniques for three-phase five level cascaded H-bridge for PV applications," *2016 IEEE International Conference on Renewable Energy Research and Applications (ICRERA)*, 2016, pp. 1173-1178.